Biosensors and Bioelectronics 124–125 (2019) 253–259

Contents lists available at ScienceDirect

Biosensors and Bioelectronics

journal homepage: www.elsevier.com/locate/bios

Improved performance Air bio-battery based on efficient oxygen supply with a gas/liquid highly-porous diaphragm cell

Koji Toma[a], Fumiya Seshima[b], Ayumi Maruyama[c], Takahiro Arakawa[a], Kazuyoshi Yano[c], Kohji Mitsubayashi[a,b,*]

[a] Department of Biomedical Devices and Instrumentation, Institute of Biomaterials and Bioengineering, Tokyo Medical and Dental University, 2-3-10 Kanda-Surugadai, Chiyoda-ku, Tokyo 101-0062, Japan
[b] Graduate School of Medical and Dental Sciences, Tokyo Medical and Dental University, 1-5-45 Yushima, Bunkyo-ku, Tokyo 113-8549, Japan
[c] School of Bioscience and Biotechnology, Tokyo University of Technology, 1404-1 Katakura, Hachioji, Tokyo 192-0982, Japan

ARTICLE INFO

Keywords:
Bio-fuel cell
Air bio-battery
Enzyme
Gas/liquid diaphragm
Glucose

ABSTRACT

Performance of a glucose-driven bio-battery was improved by enhancing electrode characteristics and oxygen supply efficiency to a cathode. The bio-battery generates electric power from glucose through three enzymatic reactions using glucose dehydrogenase, diaphorase and bilirubin oxidase. A flexible and thin Pt electrode was employed instead of a glassy carbon (GC) electrode on which enzymes, a coenzyme, and mediators were immobilized by layer-by-layer method. The maximum current and power densities of the constructed bio-battery were 257 ± 22 μA/cm^2 and 86 ± 3 μW/cm^2, respectively, in 5 mM glucose solution. In addition, a newly designed compact gas/liquid diaphragm cell, which allowed to reduce the internal resistance by shortening the anode-cathode distance and enhance oxygen supply to a cathode using a highly-porous cotton mesh diaphragm, was implemented to the bio-battery to develop a high-performance Air bio-battery. As a result, improved Air bio-battery showed the maximum current and power densities of 451 ± 27 μA/cm^2 and 162 ± 7 μW/cm^2, which was 3.6-fold improvement from the previous GC electrode-based bio-battery. In addition, continuous operation for 210 min revealed high stability of power generation as it decreased by 3.3% at the end of operation. Additional supply of oxygen to a cathode exhibited proportional increase of the power density to the oxygen concentration, which demonstrates a promising potential of Air bio-battery for a high-performance and continuous powering device.

1. Introduction

In recent years, miniaturization and diversification of medical and healthcare devices have been progressing, and technology of powering these devices has been the subject of increasing research effort. Particularly, the devices with low energy consumption such as wearable or implantable devices require constant powering (Bonfiglio and De Rossi, 2011; Khan et al., 2016). Conventional lithium-ion or lithium-iodide batteries, however, need regular charging or replacement. Energy harvesting technology has been attracting a great attention because it is able to convert ambient small energy, e.g., light, vibration, sound and chemical energy to electric power (Pfenniger et al., 2014; Sodano et al., 2004; Thielen et al., 2017; Zurbuchen et al., 2013). A bio-fuel cells is one of the energy harvesters and appears promising because it is able to produce electrical energy from redox reaction of biological substances, e.g., glucose which is constantly available from human body fluids, by utilizing biocatalysts—enzymes (Cosnier et al., 2014; Leech et al., 2012). There have been some reports of bio-batteries aiming at the use in or on living organisms (Southcott et al., 2013; Valdés-Ramírez et al., 2014): Reid et al. (2015) implemented a bio-battery in a contact lens and achieved power generation of 8.01 μW/cm^2 by tear lactate; Cadet et al. (2016) reported a bio-battery which could work in a whole human blood and showed the maximum power density of 129 μW/cm^2 at 8.22 mM glucose; Zebda et al. (2013) developed an implantable bio-battery, and demonstrated power generation of 193.5 μW/cm^2 in the abdominal cavity of a rat); MacVittie et al. (2013) or Schwefel et al. (2014) demonstrated power generation by bio-batteries in a lobster or an insect in-vivo. Some studies improved power density using nanomaterials which allowed to enhance electron transfer efficiency between enzymes and electrodes (Abreu et al., 2017; Coman

* Corresponding author at: Department of Biomedical Devices and Instrumentation, Institute of Biomaterials and Bioengineering, Tokyo Medical and Dental University, 2-3-10 Kanda-Surugadai, Chiyoda-ku, Tokyo 101-0062, Japan.
E-mail address: m.bdi@tmd.ac.jp (K. Mitsubayashi).

https://doi.org/10.1016/j.bios.2018.09.091
Received 30 June 2018; Received in revised form 6 September 2018; Accepted 27 September 2018
Available online 28 September 2018
0956-5663/

et al., 2008; Gao et al., 2007; Miyake et al., 2009; Osman et al., 2011). For example, Xu *et al.* and Ogawa *et al.* reported textile-based electrodes made conductive by carbon nanotubes. They showed stable electric properties even stretched, twisted, or wrapped form. In addition, holes in the textiles enabled efficient transport of oxygen (Ogawa et al., 2015; Xu et al., 2018). Despite of such advantages of electrodes exploiting nanomaterials, the potential health risks of nanomaterials remain unsolved, and therefore use of nanomaterials should be avoided in medical devices until toxicity of nanomaterials is thoroughly cleared.

Recently we developed a gas/liquid diaphragm cell for efficiently providing oxygen from the atmosphere, and the diaphragm cell was implemented to develop Air bio-battery (Arakawa et al., 2018). However, the generated power was not sufficient to drive devices with low power consumption, which typically require from a few to tens of mW. In this work, we improved Air bio-battery by optimizing an electrode material and an enzyme immobilization method. Also, as oxygen-limited reaction control at a cathode remains to be a bottleneck for further improvement (Cosnier et al., 2016), we fabricated a new gas/liquid diaphragm cell by a 3D printer which employed a highly-porous diaphragm to enhance oxygen supply to a cathode and shortened the electrodes distance in order to reduce internal resistance.

2. Experimental

2.1. Fabrication of anode and cathode

A bio-battery was designed to generate electric power using glucose which is a typical biological substance. Fig. 1a shows a configuration of the bio-battery and enzymatic reactions used for anode and cathode. In the anode, a cascade catalytic reaction with glucose dehydrogenase (GDH, Toyobo, Japan) and diaphorase (Dp, Oriental Yeast, Japan) was employed. Oxidized form of nicotinamide adenine dinucleotide (NAD^+)-dependent GDH catalyzed a reaction of glucose to produce reduced form of NAD (NADH, Oriental Yeast, Japan) and hydrogen ion. As it needs a large overpotential to take an electron from oxidation of NADH, Dp was used to catalyze NADH oxidation, resulting in production of NAD^+, hydrogen ion, and electrons. In the cathode, bilirubin oxidase (BOD, Amano Enzyme, Japan) was used to catalyze a redox reaction of hydrogen ion and electron, which were produced in anode, and dissolved oxygen to produce water.

As an electrode material, platinum (Pt) and glassy carbon (GC) were compared. Pt electrode has an advantage of low electrical resistivity while GC shows a wide potential window. Pt electrode was fabricated by sputtering Pt on a thin and flexible polytetrafluoroethylene (PTFE, pore size of 0.22 μm, thickness of 150 μm, Milliporer, USA) membrane, followed by O_2 plasma treatment (Aiplasma, Panasonic Electric Works, Japan) over the electrode surface (Fig. 1b). Finally, a part between a reaction and terminal areas of the Pt electrode was insulated using a thin film of polydimethylsiloxane (PDMS, SILPOT 184, Toray Dow Corning, USA). The PDMS film was prepared by mixing base elastomer and curing agent at a 9: 1 (m/m) ratio, followed by degassing the mixture using a planetary centrifugal mixer. GC electrode with outer and inner diameters of 6 mm and 1.6 mm, respectively, was purchased from BAS (Japan). A surface of GC electrode was polished (PK-3 Electrode Polishing kit, ALS, Japan) before the use.

To characterize Pt and GC electrodes, cyclic voltammetry was taken place in the potential range from −200 to + 600 mV (vs. Ag/AgCl) at the scan rate of 20 mV/s using a potentiostat (2450-EC, Keithley, USA) and a three-electrode system (Pt counter and Ag/AgCl reference electrodes). In experiment, Pt or GC working electrode was immersed together with the counter and reference electrodes in 1 mM $K_3[Fe(CN)_6]$ solution [(Wako, Japan) in a phosphate buffer solution (PB, 50 mM, pH 7)], and then redox currents of each electrode were determined.

2.2. Immobilization of enzymes, mediators, and a coenzyme on the electrodes

Methods of immobilizing enzymes, mediators, and a coenzyme were investigated. On the anode, enzymes (GDH and Dp), a coenzyme (NADH) and a mediator (vitamin K_3) (VK_3, Nacalai Tesque, Japan) were applied; on the cathode, an enzyme (BOD) and a mediator ($K_3[Fe(CN)_6]$) were used. Fig. 1c illustrates four candidate methods: (i) layer-by-layer (LbL) method, (ii) LbL on a self-assembled monolayer (SAM/LbL), (iii) entrapment using polymers, and (iv) cross-linking. In the LbL method, a cationic polymer (poly(diallyldimethylammonium chloride), PDDA, Polysciences, Taiwan) and an anionic polymer (poly(sodium 4-styrenesulfonate), PSS, Sigma-Aldrich, Japan) were used to sandwich the enzymes, mediators and a coenzyme by electrostatic interaction. The isoelectric points of all enzymes (GDH: 4.5, Dp: 4.2, BOD: 4.1) were below pH of the used buffer solution, and thus the enzymes were negatively charged and easily adsorbed to PDDA. For an anode, solutions of PDDA of 2 wt%, VK_3 of 1.5 mol/cm^2, Dp of 255 units/cm^2, NADH of 4.6 mol/cm^2, GDH of 255 units/cm^2, and PSS of 2 wt% were applied to a Pt electrode surface in this order. The electrode was dried at 40 °C in an incubator (I-Cover, As One, Japan) for 10 min after each solution was dropped. For a cathode, similar process was undertaken except that $K_3[Fe(CN)_6]$ of 5.1 mol/cm^2 and BOD of 6.6 units/cm^2 were used instead of VK_3, Dp, NADH, and GDH. Note that the same concentrations of enzymes, a coenzyme and mediators were used throughout the four methods. In the SAM/LbL method, a Pt electrode was immersed in 2-mercaptoethanesulfonic acid sodium salt (MESNA, Tokyo Chemical Industry, Japan, 1 mM in ethanol) solution for 1 h to make the Pt surface negatively charged. Then the same process of LbL formation beginning with PDDA adsorption was taken place on the SAM-modified electrode surface.

In the entrapment method, photocrosslinkable polymer (PVA-SbQ, Biosurfine SPH, Toyo Gosei, Japan) and a copolymer of 2-methacryloyloxyethyl phosphorylcholine and 2-ethyl-hexyl methacrylate (PMEH) synthesized in-house (Kudo et al., 2008) were used for anode and cathode, respectively. The reason to use different polymers for the anode and cathode was because ethanol, a solvent for PMEH, denatured GDH, and salt used as a stabilizer of BOD caused aggregation of PVA-SbQ. For an anode, a mixed solution of PVA-SbQ of 6.25 mg/cm^2, GDH, Dp, NADH and VK_3 were applied to a Pt electrode, followed by being dried in a dark and cool (4 °C) place. Then the electrode was exposed to UV-light (wavelength of 352 nm, 6.4 mW/cm^2) for 5 min to cure PVA-SbQ, followed by being dried in the dark and cool place for 12 h. For a cathode, a mixed solution of $K_3[Fe(CN)_6]$ and BOD and 5 wt% PMEH were applied to the Pt electrode, followed by being dried in the dark and cool place for 1 h.

In the cross-linking method, glutaraldehyde (GA, Wako, Japan) was used as a cross-linker. Also, bovine serum albumin (BSA, Wako, Japan) was used to prevent overcross-linking of enzymes. First, a mixed solution of BSA of 4.5 wt% and the same enzymes, coenzyme and mediators used in the other methods was applied to a Pt electrode. Afterwards, 4.5 wt% GA solution was dropped on the Pt electrode, and the electrode was dried in the dark and cool place for 1 h.

Now a bio-battery was constructed using the prepared anode and cathode and characterized in 5 mM (90 mg/dL) glucose solution which corresponds to the blood glucose level. Output potential was measured using an electrometer (8240, ADC, Japan) while varying a resistance between the anode and cathode. The power generation characteristics was assessed with a power density, which was calculated from the resistance and corresponding output potential.

2.3. Construction of compact Air bio-battery

In a previous work, we reported Air bio-battery, a normally-aspirated bio-battery, with a gas/liquid porous diaphragm cell. The diaphragm cell took oxygen from the air to improve oxygen supply to the

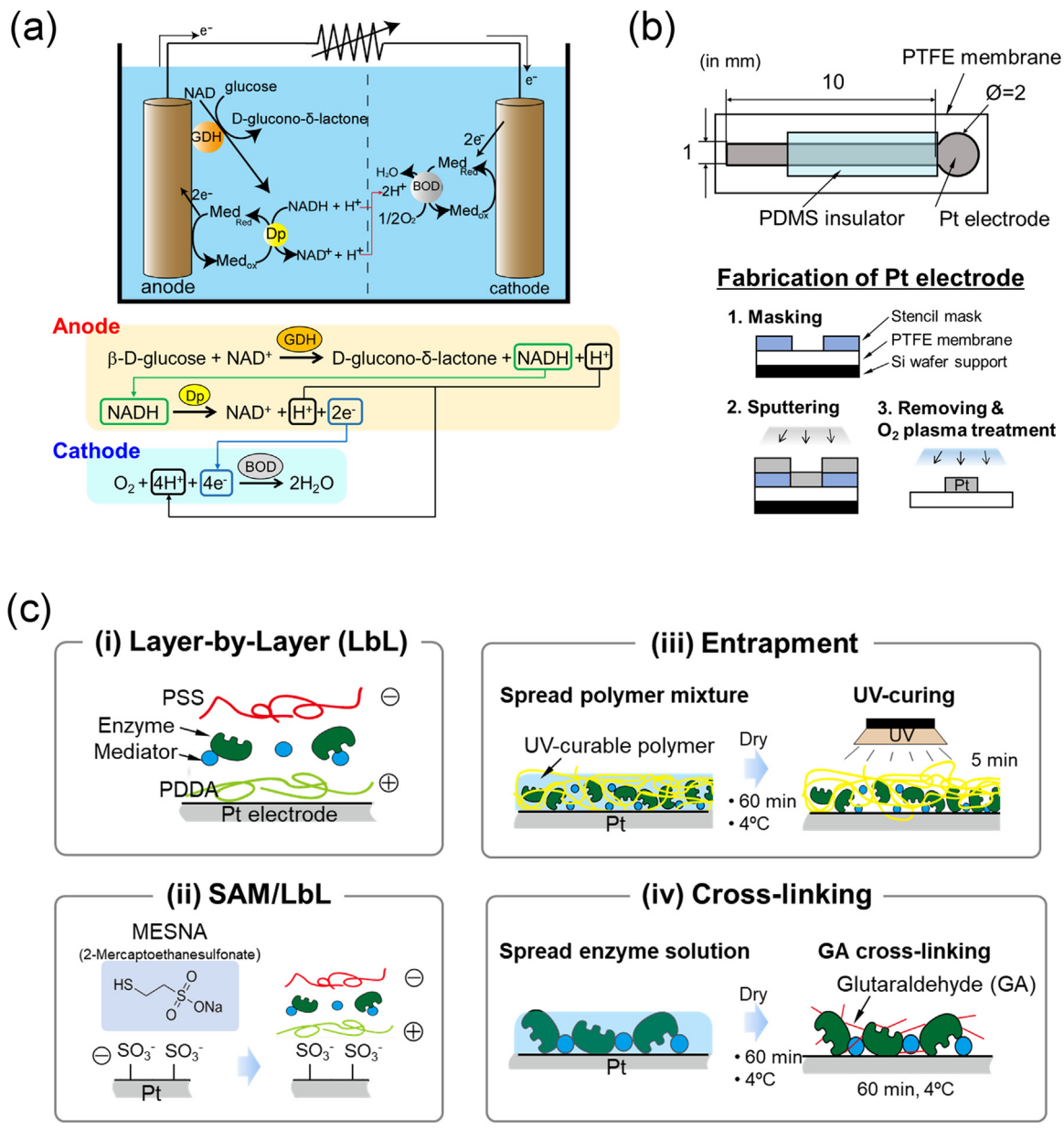

Fig. 1. (a) Schematic illustration of a bio-battery and enzymatic reactions used for power generation. (b) Pt electrode used in a bio-battery (upper) and fabrication procedure of a Pt electrode (lower). (c) Various immobilization methods of enzymes, a coenzyme and mediators. Pt, platinum; PTFE, Polytetrafluoroethylene; PDMS, Polydimethylsiloxane GDH, glucose dehydrogenase; Dp, diaphorase; BOD, bilirubin oxidase; NAD^+, oxidized form of nicotinamide adenine dinucleotide (NAD); NADH, reduced form of NAD.

cathode (Arakawa et al., 2018), which resulted in the improvement of power generation capability of the bio-battery. In this study, such Air bio-battery was improved in three points: first, a 1.5-fold thinner gas/liquid diaphragm with 3000-fold larger pore size was employed to enhance oxygen supply efficiency. A previously used diaphragm, PTFE membrane (pore size of 0.22 μm, thickness of 150 μm, Millipore, USA), was replaced with a cotton mesh (pore size of 700 μm, thickness of 100 μm) whose both sides were made hydrophobic so as to prevent liquid leak; second, electrode distance was made one order of magnitude shorter than the previous Air bio-battery (from 25 mm to 2.5 mm) (Fig. 2). It could reduce internal resistance and thereby improve the mobility of a hydrogen ion; third, the size of the cell was made compact (height of 22 mm, diameter of 40 mm), and the volume of the cell became 1/77 of the previous Air bio-battery. The new Air bio-battery had a cylindrical shape and was composed of a lid and a body. They were made of acrylonitrile-butadiene-styrene (ABS) resin, and fabricated by a 3D printer (uPrint SE plus, Stratasys, USA). The anode was attached to a bottom of the body by O-ring. The cathode was attached under the cotton mesh by O-ring in such a way that an enzyme-immobilized side of the electrode faced to the cotton mesh. After fabrication, the new Air bio-battery was filled with 5 mM glucose solution and characterized in the same way with the bio-battery.

3. Results and discussion

3.1. Characteristics of electrodes

Fig. 3a shows cyclic voltammograms of a Pt electrode with O_2 plasma treatment and a GC electrode in 1 mM $K_3[Fe(CN)_6]$ solution (pH7.0). Both oxidation and reduction peak currents were higher in the Pt electrode while these were observed at the similar potentials (oxidation: 236 mV, reduction: 163 mV). The redox peak current densities

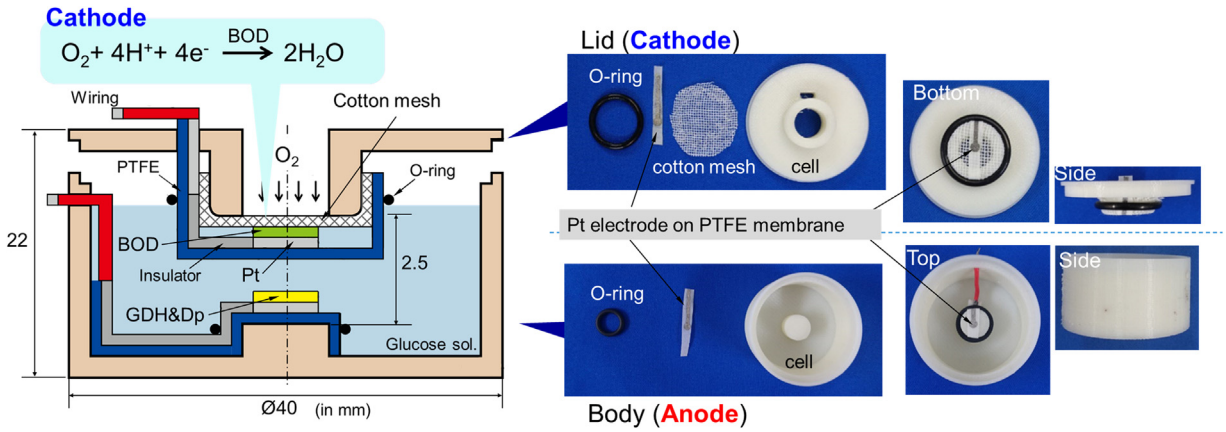

Fig. 2. Schematic illustration and images of improved performance Air bio-battery.

are summarized in Fig. 3b. Compared to the GC electrode, the Pt electrode on a hydrophilic PTFE showed about 1.5-fold higher current densities (oxidation: 207 ± 4 μA/cm^2, reducition: 205 ± 14 μA/cm^2). In addition, O2 plasma treatment resulted in 2.7-fold improvement in the current densities for the Pt electrode. This may be attributed to enhancement of wettability of both Pt electrode and PTFE membrane by O_2 plasma treatment. Based on these superior electrochemical characteristics, we decided to use a plasma-treated Pt electrode for a bio-battery in subsequent experiments. This CV data also determined the mid-peak potentials of $K_3[Fe(CN)_6]$ in solution to be of 200 mV, which was lower than that of VK_3 (-0.19 mV) (Togo et al., 2007).

The peak redox current densities of electrodes with various enzyme immobilization methods are shown in Fig. 4. For an anode, an enzyme-immobilized Pt electrode was immersed in 50 mM glucose solution, and the peak oxidation current was determined from a cyclic voltammogram (Supplemental Fig. 1a). Among four different methods, the SAM/LbL method resulted in the highest oxidation current density (1231 ± 70 μA/cm^2) (Fig. 4a). However, a shift of the oxidation potential to the positive direction was observed because the negatively charged Pt surface by the SAM could cause electrostatic repulsion, which may have caused inhibition of electron transfer (Supplemental Fig. 1a). This side effect is expected to be improved by a thiol with a positively charged functional group, e.g., amino groups, instead of MESNA. This oxidation potential shift may lead to impairing the open circuit voltage of the bio-battery that is determined by the difference between oxidation potential of an anode and reduction potential of a cathode. Therefore, we chose the LbL method for anode that showed the second largest peak oxidation current density (911 ± 74 μA/cm^2). For cathode, the prepared enzyme-immobilized Pt electrode was immersed in PB, and cyclic voltammetry was taken place (Supplemental Fig. 1b). The results showed that SAM/LbL method exhibited the highest reduction current (1383 ± 65 μA/cm^2) (Fig. 4b). In this case, the shift of the reduction potential was not observed. According to the above results, we decided to use the SAM/LbL method for preparing a cathode.

Now, concentrations of enzymes, a coenzyme and mediators were optimized. The composition concentrations mentioned above, (GDH of 255 units/cm^2, Dp of 255 units/cm^2, NADH of 4.6 mol/cm^2, VK_3 of 1.5 mol/cm^2 for anode; BOD, 6.6 units/cm^2, K_3 $[Fe(CN)_6]$, 5.1 mol/cm^2 for cathode) were used as the standard value, and the current peak density was determined for each relative concentration by cyclic voltammetry (Supplemental Fig. 2). For the anode, the peak oxidation current density increased with increasing the relative composition concentration and peaked at the relative concentration of 200% (1383 ± 114 μA/cm^2), which was 1.9-fold higher than the current at the standard concentration (694 ± 81 μA/cm^2) (Fig. 5a). Decrease in the current above this concentration may be because local pH decrease nearby the electrode due to excessive oxidation degraded enzyme activity. For the cathode, the peak reduction current density improved by a factor 1.3 from the standard concentration (1581 ± 154 μA/cm^2) at the relative concentration of 125% (1743 ± 176 μA/cm^2) (Fig. 5b). Decrease in the current above this concentration may be due to local pH increase around the electrode, which was caused by protons

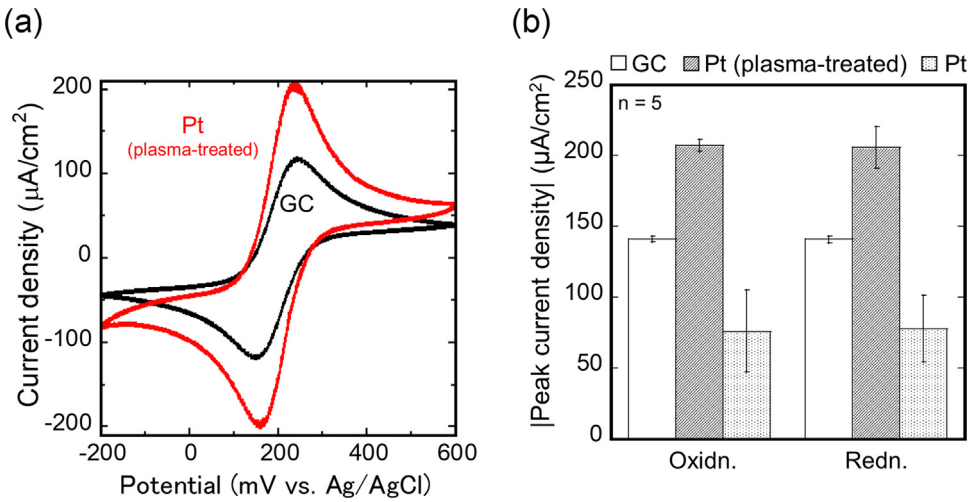

Fig. 3. (a) Typical cyclic voltammograms of (black) a GC and (red) a plasma-treated Pt electrodes in 1 mM $K_3[Fe(CN)_6]$ solution (pH7.0) at a scan rate of 20 mV/s. (b) Redox peak current densities of (blank) the GC, (hatched) the plasma-treated Pt and (dotted) the non-treated Pt electrodes.

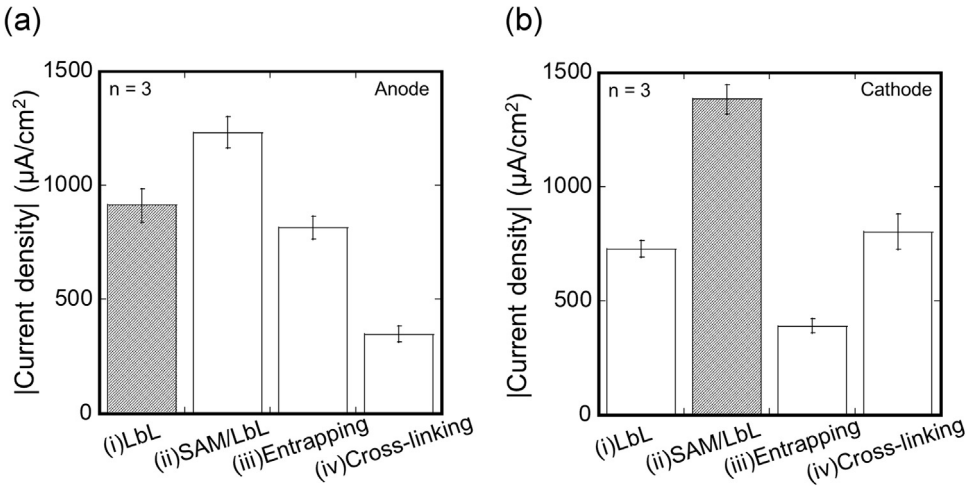

Fig. 4. Peak current densities of (a) oxidation for an anode and (b) reduction for a cathode with enzyme, coenzyme and mediator which were immobilized by various methods: (i) LbL, (ii) SAM/LbL, (iii) entrapment, and (iv) cross-linking. Scan speed, 20 mV/s in (a) 50 mM glucose solution and (b) PB.

consumption and resulted in degradation of enzyme activity. According to the results above, we chose the relative concentration of 200% for the anode, and 125% for the cathode in subsequent experiments.

3.2. Assessment of the new Air bio-battery

A bio-battery was constructed using the electrodes fabricated under the above determined conditions. When the anode and cathode were immersed in 5 mM glucose solution, a concentration corresponding to blood glucose level, the electromotive force was generated between two electrodes, and change in the output potential was observed (Fig. 6a). The obtained maximum power and current densities of the bio-battery were of 86 ± 3 μW/cm2 and 257 ± 22 μA/cm^2 (n = 3), respectively. Compared to the previous GC electrode-based bio-battery (45 μW/cm^2) (Arakawa et al., 2018), 1.9-fold improvement in the maximum power density was achieved by employing Pt electrode and optimizing the enzyme immobilization. Here, the reason why the improvement in the power density was not as high as seen in the oxidation and reduction current densities at the electrodes may be due to reaction control by shortage of dissolved oxygen at the cathode. Therefore, we expected that the power generation could be further improved by enhancing oxygen supply to the cathode.

The constructed Air bio-battery with a hydrophobic cotton mesh gas/liquid diaphragm, which was expected to improve oxygen supply by normal aspiration, was characterized. It showed the maximum power density of 162 ± 7 μW/cm^2 (n = 3), which was 1.9-fold and 2.3-fold higher than that of the Pt electrode-based bio-battery and the previous Air bio-battery with GC electrode (70.7 μW/cm^2) (Arakawa et al., 2018). Even compared to other works, the presented new Air bio-battery showed a relatively high power density. For example, Pankratov *et al.*, reported a transparent and flexible nanostructured-biofuel cell and achieved the power density of 0.6 μW/cm^2 with 5 mM glucose (Pankratov et al., 2015). Karaśkiewicz*et al.*, developed a biofuel cell with carbon nanotube composit bioelectrodes. They achieved the power density of 131 μW/cm^2 with 80 mM glucose (Karaśkiewicz et al., 2012). The result also indicates that a structure of the compact Air bio-battery and a cotton mesh with a larger pore size allows to further advance the battery characteristics in addition to exploiting Pt electrode.

To investigate whether more oxygen supply influences on the power generation capability of Air bio-battery, oxygen with a 1.3-fold higher concentration (26.8%) than the atmosphere (20.9%) was applied to the cotton mesh diaphragm of Air bio-battery using an oxygen air charger (MS-X1, Panasonic, Japan). The result showed that the maximum power density was improved by a factor of 1.3 (211 ± 6 μW/cm^2), which was proportional to the increase in the oxygen concentration. Therefore, it is anticipated that about 5-fold improvement (about 800 μW/cm^2) in the power density could be realized if the oxygen concentration around the cathode were increased to 100%. The oxygen concentration dependency of the power generation also implies that a textile-based electrode should be useful because holes of the textile are expected to enhance oxygen transport. In such a case, enzymes can be entrapped on the textile using polymers as we reported in other works

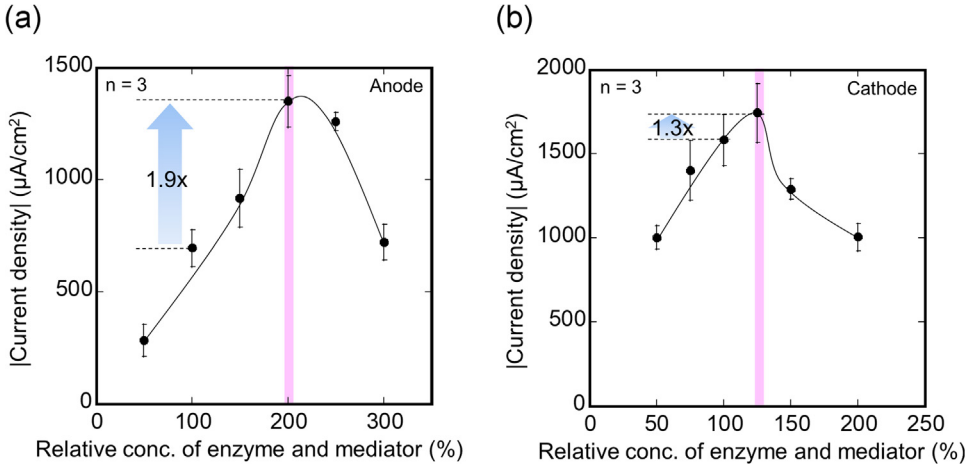

Fig. 5. Influence of concentration of enzyme, coenzyme and mediator on the peak oxidation and reduction current densities of (a) anode and (b) cathode, respectively. Standard concentration: (anode) GDH, 255 units/cm^2; Dp, 255 units/cm^2; NADH, 4.6 mol/cm^2; VK_3, 1.5 mol/cm^2; (cathode) BOD, 6.6 units/cm^2; $K_3[Fe(CN)_6]$, 5.1 mol/cm^2. Scan speed, 20 mV/s in (a) 50 mM glucose solution and (b) PB.

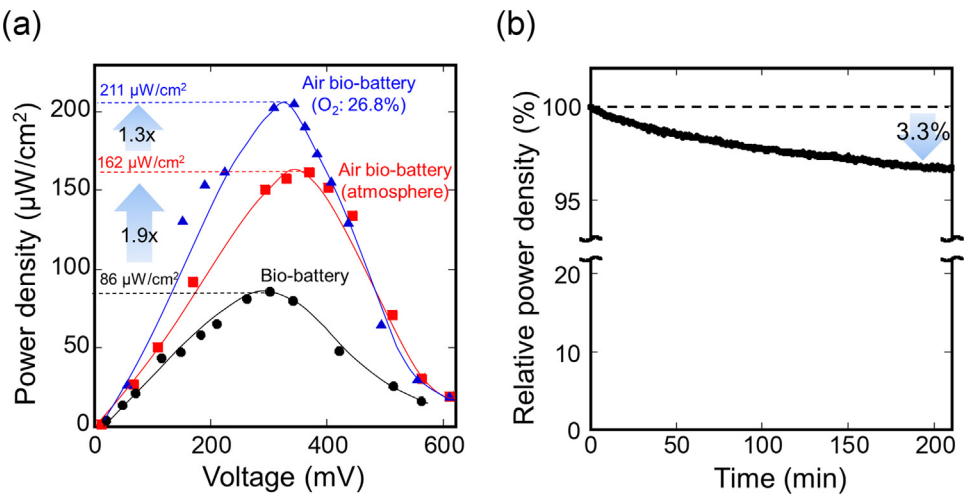

Fig. 6. (a) Generated power densities by (•) a bio-battery, (■) Air bio-battery in atmosphere (20.9% O_2) and (▲) in 26.8% O_2. (b) Time course of the maximum power density by improved performance Air bio-battery. Sample solution: 5 mM glucose solution.

(Arakawa et al., 2017; Iitani et al., 2018).

Finally, a battery lifetime was also investigated. Fig. 6b shows a time-course of the relative maximum power density of Air bio-battery while 26.8% oxygen was supplied. The generated power gradually decreased, and the decrement was of 3.3% at 210 min. This may be attributed to lack of glucose in the solution after continuous consumption of glucose through the power generation.

4. Conclusion

In this study, performance of Air bio-battery was improved by optimizing electrodes and constructing a compact gas/liquid diaphragm cell with a highly-porous cotton mesh diaphragm. A thin and flexible Pt electrode which showed superior electrochemical characteristics to GC electrode was adopted as an electrode. Enzymes, a coenzyme, and mediators were then immobilized on the Pt electrode using LbL method for an anode and SAM/LbL method for a cathode. After the optimization of the electrode, the power generation capability of the bio-battery was improved by a factor of 1.9 (86 μW/cm^2), compared to a previous bio-battery using a GC electrode. Further improvement of the power generation capability was achieved by enhancing oxygen supply to a cathode where the reaction control had occurred due to shortage of dissolved oxygen in solution. A hydrophobic cotton mesh with 3000-fold larger pore size than a previously used PTFE membrane was employed as a diaphragm. As a result of improved normal aspiration as well as the shortened electrode distance, 3.6-fold improvement of the maximum power density (162 μW/cm^2) was achieved from the previous GC electrode-based bio-battery. An experiment in which higher concentration of oxygen was supplied to the cathode of Air bio-battery revealed proportional increase of the maximum power density to the oxygen concentration. This indicates that there is potential in Air bio-battery for further 5-fold improvement from this work if oxygen concentration at the cathode could be increased to 100%. According to these results along with a fact that this battery was able to be continuously operated for a long time without substantial degradation, Air bio-battery is a promising candidate of a power source for healthcare or medical devices which consumes low power and needs to work continuously.

Acknowledgments

This work was partly supported by a grant from Japan IDDM network and the Ministry of Education, Culture, Sports, Science and Technology (MEXT, Japan) Special Funds for “Cooperative Research Project of Research Center for Biomedical Engineering”.

Appendix A. Supplementary material

Supplementary data associated with this article can be found in the online version at doi:10.1016/j.bios.2018.09.091.

References

Abreu, C., Nedellec, Y., Gross, A.J., Ondel, O., Buret, F., Goff, A., Le, Holzinger, M., Cosnier, S., 2017. Assembly and stacking of flow-through enzymatic bioelectrodes for high power glucose fuel cells. ACS Appl. Mater. Interfaces 9, 23836–23842. https://doi.org/10.1021/acsami.7b06717.

Arakawa, T., Sato, T., Iitani, K., Toma, K., Mitsubayashi, K., 2017. Fluorometric biosniffer camera “Sniff-cam” for direct imaging of gaseous ethanol in breath and transdermal vapor. Anal. Chem. 89, 4495–4501. https://doi.org/10.1021/acs.analchem.6b04676.

Arakawa, T., Xie, R., Seshima, F., Toma, K., Mitsubayashi, K., 2018. Air bio-battery with a gas/liquid porous diaphragm cell for medical and health care devices. Biosens. Bioelectron. 103, 171–175. https://doi.org/10.1016/j.bios.2017.12.016.

Bonfiglio, A., De Rossi, D., 2011. Wearable Monitoring Systems. pp. 1–296. https://doi.org/10.1007/978-1-4419-7384-9.

Cadet, M., Gounel, S., Stines-Chaumeil, C., Brilland, X., Rouhana, J., Louerat, F., Mano, N., 2016. An enzymatic glucose/O_2biofuel cell operating in human blood. Biosens. Bioelectron. 83, 60–67. https://doi.org/10.1016/j.bios.2016.04.016.

Coman, V., Vaz-Domínguez, C., Ludwig, R., Harreither, W., Haltrich, D., De Lacey, A.L., Ruzgas, T., Gorton, L., Shleev, S., 2008. A membrane-, mediator-, cofactor-less glucose/oxygen biofuel cell. Phys. Chem. Chem. Phys. 10, 6093–6096. https://doi.org/10.1039/b808859d.

Cosnier, S., Gross, A.J., Le Goff, A., Holzinger, M., 2016. Recent advances on enzymatic glucose/oxygen and hydrogen/oxygen biofuel cells: achievements and limitations. J. Power Sources 325, 252–263. https://doi.org/10.1016/j.jpowsour.2016.05.133.

Cosnier, S., Le Goff, A., Holzinger, M., 2014. Towards glucose biofuel cells implanted in human body for powering artificial organs: review. Electrochem. Commun. 38, 19–23. https://doi.org/10.1016/j.elecom.2013.09.021.

Gao, F., Yan, Y., Su, L., Wang, L., Mao, L., 2007. An enzymatic glucose/O_2biofuel cell: preparation, characterization and performance in serum. Electrochem. Commun. 9, 989–996. https://doi.org/10.1016/j.elecom.2006.12.008.

Iitani, K., Sato, T., Naisierding, M., Hayakawa, Y., Toma, K., Arakawa, T., Mitsubayashi, K., 2018. Fluorometric sniff-cam (Gas-Imaging System) Utilizing alcohol dehydrogenase for imaging concentration distribution of acetaldehyde in breath and transdermal vapor after drinking. Anal. Chem. 90, 2678–2685. https://doi.org/10.1021/acs.analchem.7b04474.

Karaśkiewicz, M., Nazaruk, E., Zelechowska, K., Biernat, J.F., Rogalski, J., Bilewicz, R., 2012. Fully enzymatic mediatorless fuel cell with efficient naphthylated carbon nanotube-laccase composite cathodes. Electrochem. Commun. 20, 124–127. https://doi.org/10.1016/j.elecom.2012.04.011.

Khan, Y., Ostfeld, A.E., Lochner, C.M., Pierre, A., Arias, A.C., 2016. Monitoring of vital signs with flexible and wearable medical devices. Adv. Mater. 28, 4373–4395. https://doi.org/10.1002/adma.201504366.

Kudo, H., Yagi, T., Chu, M.X., Saito, H., Morimoto, N., Iwasaki, Y., Akiyoshi, K., Mitsubayashi, K., 2008. Glucose sensor using a phospholipid polymer-based enzyme immobilization method. Anal. Bioanal. Chem. 391, 1269–1274. https://doi.org/10.1007/s00216-007-1824-8.

Leech, D., Kavanagh, P., Schuhmann, W., 2012. Enzymatic fuel cells: recent progress. Electrochim. Acta 84, 223–234. https://doi.org/10.1016/j.electacta.2012.02.087.

MacVittie, K., Halámek, J., Halámková, L., Southcott, M., Jemison, W.D., Lobel, R., Katz, E., 2013. From “cyborg” lobsters to a pacemaker powered by implantable biofuel cells. Energy Environ. Sci. 6, 81–86. https://doi.org/10.1039/c2ee23209j.

Miyake, T., Oike, M., Yoshino, S., Yatagawa, Y., Haneda, K., Kaji, H., Nishizawa, M., 2009. Biofuel cell anode: nad+/glucose dehydrogenase-coimmobilized ketjenblack

electrode. Chem. Phys. Lett. 480, 123–126. https://doi.org/10.1016/j.cplett.2009.08.075.
Ogawa, Y., Takai, Y., Kato, Y., Kai, H., Miyake, T., Nishizawa, M., 2015. Stretchable biofuel cell with enzyme-modified conductive textiles. Biosens. Bioelectron. 74, 947–952. https://doi.org/10.1016/j.bios.2015.07.063.
Osman, M.H., Shah, A.A., Walsh, F.C., 2011. Recent progress and continuing challenges in bio-fuel cells. Part I: enzymatic cells. Biosens. Bioelectron. 26, 3087–3102. https://doi.org/10.1016/j.bios.2011.01.004.
Pankratov, D., Sundberg, R., Sotres, J., Maximov, I., Graczyk, M., Suyatin, D.B., González-Arribas, E., Lipkin, A., Montelius, L., Shleev, S., 2015. Transparent and flexible, nanostructured and mediatorless glucose/oxygen enzymatic fuel cells. J. Power Sources 294, 501–506. https://doi.org/10.1016/j.jpowsour.2015.06.041.
Pfenniger, A., Vogel, R., Koch, V.M., Jonsson, M., 2014. Performance analysis of a miniature turbine generator for Intracorporeal energy harvesting. Artif. Organs 38. https://doi.org/10.1111/aor.12279.
Reid, R.C., Minteer, S.D., Gale, B.K., 2015. Contact lens biofuel cell tested in a synthetic tear solution. Biosens. Bioelectron. 68, 142–148. https://doi.org/10.1016/j.bios.2014.12.034.
Schwefel, J., Ritzmann, R.E., Lee, I.N., Pollack, A., Weeman, W., Garverick, S., Willis, M., Rasmussen, M., Scherson, D., 2014. Wireless communication by an autonomous Self-powered Cyborg insect. J. Electrochem. Soc. 161, H3113–H3116. https://doi.org/10.1149/2.0171413jes.
Sodano, H.A., Inman, D.J., Park, G., 2004. A review of power harvesting from vibration using piezoelectric materials. Shock Vib. Dig. 36, 197–205. https://doi.org/10.1177/0583102404043275.
Southcott, M., MacVittie, K., Halámek, J., Halámková, L., Jemison, W.D., Lobel, R., Katz, E., 2013. A pacemaker powered by an implantable biofuel cell operating under conditions mimicking the human blood circulatory system-battery not included. Phys. Chem. Chem. Phys. 15, 6278–6283. https://doi.org/10.1039/c3cp50929j.
Thielen, M., Sigrist, L., Magno, M., Hierold, C., Benini, L., 2017. Human body heat for powering wearable devices: from thermal energy to application. Energy Convers. Manag. 131, 44–54. https://doi.org/10.1016/j.enconman.2016.11.005.
Togo, M., Takamura, A., Asai, T., Kaji, H., Nishizawa, M., 2007. An enzyme-based microfluidic biofuel cell using vitamin K3-mediated glucose oxidation. Electrochim. Acta 52, 4669–4674. https://doi.org/10.1016/j.electacta.2007.01.067.
Valdés-Ramírez, G., Li, Y.C., Kim, J., Jia, W., Bandodkar, A.J., Nuñez-Flores, R., Miller, P.R., Wu, S.Y., Narayan, R., Windmiller, J.R., Polsky, R., Wang, J., 2014. Microneedle-based self-powered glucose sensor. Electrochem. Commun. 47, 58–62. https://doi.org/10.1016/j.elecom.2014.07.014.
Xu, S., Yao, Y., Guo, Y., Zeng, X., Lacey, S.D., Song, H., Chen, C., Li, Y., Dai, J., Wang, Y., Chen, Y., Liu, B., Fu, K., Amine, K., Lu, J., Hu, L., 2018. Textile inspired lithium–oxygen battery cathode with decoupled oxygen and electrolyte pathways. Adv. Mater. 30, 1–8. https://doi.org/10.1002/adma.201704907.
Zebda, A., Cosnier, S., Alcaraz, J.P., Holzinger, M., Le Goff, A., Gondran, C., Boucher, F., Giroud, F., Gorgy, K., Lamraoui, H., Cinquin, P., 2013. Single glucose biofuel cells implanted in rats power electronic devices. Sci. Rep. 3, 1–5. https://doi.org/10.1038/srep01516.
Zurbuchen, A., Pfenniger, A., Stahel, A., Stoeck, C.T., Vandenberghe, S., Koch, V.M., Vogel, R., 2013. Energy harvesting from the beating heart by a mass imbalance oscillation generator. Ann. Biomed. Eng. 41, 131–141. https://doi.org/10.1007/s10439-012-0623-3.